JCI The Journal of Clinical Investigation

Lymphatic impairment leads to pulmonary tertiary lymphoid organ formation and alveolar damage

Hasina Outtz Reed, … , Wayne W. Hancock, Mark L. Kahn

J Clin Invest. 2019. https://doi.org/10.1172/JCI125044.

Research In-Press Preview Pulmonology Vascular biology

Graphical abstract

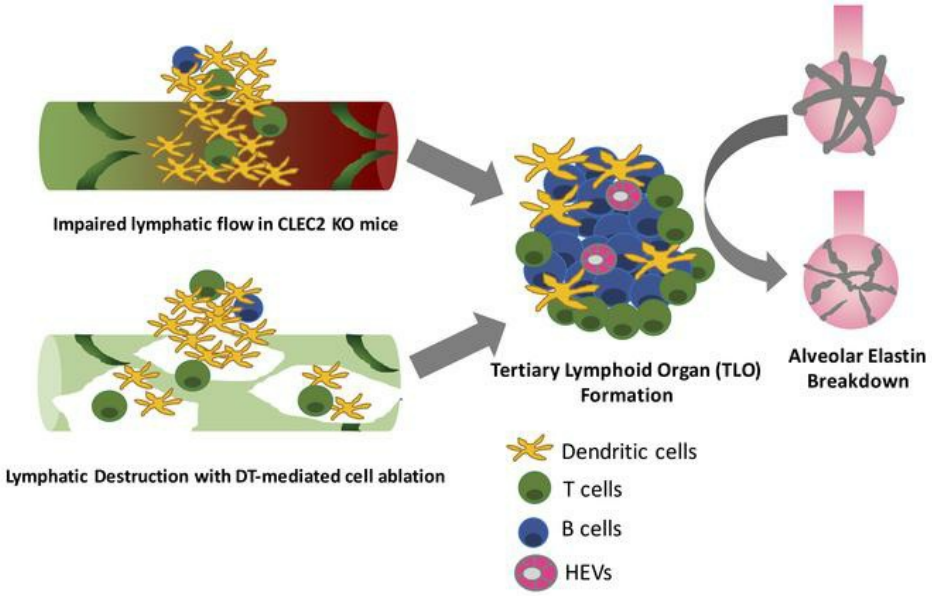

Find the latest version:

https://jci.me/125044/pdf

Lymphatic impairment leads to pulmonary tertiary lymphoid organ formation and alveolar damage

Hasina Outtz Reed[1,2], Liqing Wang[3], Jarrod Sonett[4], Mei Chen[2], Jisheng Yang[2], Larry Li[2], Petra Aradi[5,6], Zoltan Jakus[5,6], Jeanine D'Armiento[4], Wayne W. Hancock[3], and Mark L. Kahn[2]

[1]Department of Medicine and Division of Pulmonary and Critical Care, University of Pennsylvania
[2]Department of Medicine and Cardiovascular Institute, University of Pennsylvania
[3]Department of Pathology and Laboratory Medicine, Division of Transplant Immunology, Children's Hospital of Philadelphia and University of Pennsylvania
[4]Department of Anesthesiology, Center for Molecular Pulmonary Disease, College of Physicians and Surgeons, Columbia University
[5]Department of Physiology, Semmelweis University School of Medicine
[6]MTA-SE "Lendület" Lymphatic Physiology Research Group of the Hungarian Academy of Sciences and the Semmelweis University

The authors have declared that no conflict of interest exists.

Abstract

The lung is a specialized barrier organ that must tightly regulate interstitial fluid clearance and prevent infection in order to maintain effective gas exchange. Lymphatic vessels are important for these functions in other organs, but their roles in the lung have not been fully defined. In the present study, we addressed how the lymphatic vasculature participates in lung homeostasis. Studies using mice carrying a lymphatic reporter allele revealed that, in contrast to other organs, lung lymphatic collecting vessels lack smooth muscle cells entirely, suggesting that forward lymph flow is highly dependent on movement and changes in pressure associated with respiration. Functional studies using CLEC2-deficient mice in which lymph flow is impaired due to loss of lympho-venous hemostasis or using inducible lung-specific ablation of lymphatic endothelial cells in a lung transplant model revealed that loss of lymphatic function leads to an inflammatory state characterized by the formation of tertiary lymphoid organs (TLOs). In addition, impaired lymphatic flow in mice resulted in hypoxia and features of lung injury that resemble emphysema. These findings reveal both a lung-specific mechanism of lymphatic physiology and a lung-specific consequence of lymphatic dysfunction that may contribute to chronic lung diseases that arise in association with TLO formation.

Introduction

The lymphatic vascular system transports fluid, immune cells, and lipids throughout the body to prevent tissue edema, facilitate adaptive immune responses, and enable efficient fat handling. The lymphatic network is typically depicted as a network of smaller lymphatic capillaries that are specialized to take up cells, protein, and fluid, as well as larger collecting lymphatics that are designed to return lymph to the venous system and facilitate immune surveillance in secondary lymphoid organs such as lymph nodes. Recent studies of the blood vascular system have highlighted molecular and structural features that contribute to organ-specific roles of these vessels such as the blood-brain barrier, liver sinusoids, and the bone marrow hematopoietic niche (1). With the exception of villus lacteals that are specialized for the uptake and transport of dietary fats, the extent to which the lymphatic vascular system exhibits similar organ-specific structure and function at other sites in the body remains unclear.

Lymphatic vessels are relatively abundant in the lung, an organ that is uniquely sensitive to edema and inflammation that may impair gas exchange. In the developing lung, lymphatic function is required to drain fluid and achieve the compliance that is necessary for neonatal lung inflation (2, 3), but the role of lymphatics in the mature lung is undefined. One proposed role of pulmonary lymphatics is to drain fluid from the lung in order to prevent pulmonary edema that would reduce gas exchange. However, in the canonical physiologic model proposed by Ernest Starling, fluid balance in the lung is maintained by a balance of hydrostatic forces that move fluid from the blood and into the interstitium with oncotic forces that move fluid from the interstitium into the blood. In this model, lymphatics are not required to maintain fluid balance, but the role of pulmonary lymphatics in lung fluid homeostasis has yet to be fully tested. Short-term studies using catheter-based approaches in large animals have attempted to investigate the function of lymphatics in the lung (4), but lymph flow is exceedingly slow compared to flow in the blood circulation (2ml/min versus 5000ml/min (5)). Thus, the consequences of changes in lymphatic function may require days to weeks to manifest.

The lung is constantly exposed to the outside environment, and must maintain both a quiescent immune state while having the ability to generate a robust immune response to pathogens in order to prevent infection. Immune cell trafficking to draining lymph nodes via the pulmonary lymphatics plays a central role in coordinating the adaptive immune response to infection and other pathogens (6, 7). Chronic inflammation is often associated with the development of tertiary lymphoid organs (TLOs), also known as inducible bronchus-associated lymphoid tissue (iBALT), which are accumulations of lymphoid cells that resemble lymph nodes in cellular content, organization, and the presence of lymphatic vessels (8, 9). Although TLOs are a hallmark of chronic lung disease (10), it is unclear why they result from such widely differing insults as chronic cigarette smoke exposure and infection. Although lymphatic vessels and lymphangiogenesis are key features of TLOs (8, 11), whether TLO formation is connected to lymphatic function is unknown. Finally, although abnormal lymphatics have been described in association with a variety of lung diseases (12), whether they are simply a consequence of the disease or whether lymphatic dysfunction actively contributes to lung injury is unknown.

To address the role of lymphatics in the adult lung, we have characterized pulmonary lymphatic anatomy and used two distinct models of impaired pulmonary lymphatic flow in the mouse: CLEC2-deficient mice in which blood obstructs the forward flow of lymph in the lung (13), and mice in which the pulmonary lymphatics have been genetically engineered to enable specific deletion following lung transplantation using diphtheria toxin. We found that pulmonary collecting lymphatics have valves but lack smooth muscle cells, a unique characteristic of these vessels that is consistent with propulsion of lymph through respiration-associated changes in thoracic pressure rather than contraction of the vessel. Functional studies demonstrate that mice with impaired pulmonary lymphatic flow are susceptible to increased pulmonary edema following lung injury, and develop pronounced leukocyte accumulation and TLO formation in the lung parenchyma even in the absence of injury. Unexpectedly, mice with TLO formation associated with impaired lymphatic flow developed hypoxia and lung injury with several features

of human emphysema. These findings identify unique physiological and pathological aspects of lymphatic function in the lung and suggest that lymphatic dysfunction may play a role in the pathogenesis of chronic lung disease.

Results

Pulmonary collecting lymphatics lack smooth muscle cell coverage

To address the specific roles of lymphatic vessels in pulmonary physiology and pathophysiology, we first carefully examined lung lymphatic vascular anatomy. The lymphatic system classically consists of both smaller primary lymphatic capillaries that take up fluid, proteins, and cells from the tissue as well as larger collecting vessels that transport lymph to lymph nodes and, ultimately, the venous system. Whereas lymph flow within lymphatic capillaries is passive, the collecting lymphatics are typically characterized by the presence of functional units known as lymphangions that actively pump lymph (14). Lymphangions consist of smooth muscle cell (SMC)-lined segments of lymphatic vessel separated by valves (15). Physiologic studies of collecting lymphatics from the limb and mesentery have demonstrated that active SMC contraction and valve activity are coordinated to create waves of forward movement of lymph (16-19). In the lung however, physiologic studies using catheter-based measurement of pulmonary lymph flow in anesthetized large animals have suggested that extrinsic forces such as changes in thoracic pressure associated with respiration may play a more central role (3, 4, 20-22).

To characterize the pulmonary lymphatic network and to compare it to better characterized lymphatic beds such as those in the gut and mesentery, we performed whole mount imaging of lungs from *Prox1-EGFP* mice in which lymphatic endothelial cells are marked by GFP expression (23). Whole mount immunostaining for smooth muscle actin (SMA) revealed complete coverage of arterial vessels and characteristic partial coverage of bronchi, but virtually no SMA staining was detected on pulmonary lymphatic vessels (Figure 1A,B). Even the largest lymphatic collecting vessels in the lung, identified by their more proximal location adjacent to large airways and blood vessels (Figure 1A) as well as by the presence of $PROX1^{hi}$ endothelial cells that mark lymphatic valves (Figure 1B), were devoid of all SMA staining. Using

conventional immunohistochemistry of lung sections, SMA staining could be seen lining airways but neither SMA nor the pericyte marker NG2 were detectable alongside lymphatic endothelium marked by VEGFR3 or LYVE1 expression (Figure 1C,D). Prior studies have reported SMA staining alongside LYVE1$^+$ endothelial cells (24), but careful analysis of LYVE1 staining revealed that unlike VEGFR3 staining, LYVE1 was readily detected in large blood vessels and capillaries in the lung and therefore does not independently serve as a specific marker of lung lymphatic vessels (Figure 1C,D and Supplemental Figure 1). Analysis of 180 distinct lung lymphatic vessels identified using VEGFR3 staining from 6 different animals revealed no associated SMA$^+$ cells (Supplemental Table 1). In contrast, collecting lymphatics in other tissues such as the skin (Figure 1E) and diaphragm (Figure 1F) exhibited robust SMC coverage in non-valvular regions, consistent with classic lymphangion anatomy (16, 19). Importantly, immunostaining of collecting lymphatic vessels in normal human lung tissue, identified by expression of the lymphatic endothelial-specific marker PODOPLANIN (25, 26), also showed a lack of lymphatic SMC coverage (Figure 1G,H). These results reveal that collecting lymphatic vessels in the lung have a unique anatomy in which the classic lymphangion is absent, and suggest that lymph flow in the lung does not rely upon intrinsic pumping of the collecting lymphatic vasculature.

Mice lacking CLEC2 exhibit abnormal pulmonary lymphatic morphology and function

To functionally address the role of lymphatic vessels in the mature lung over time, we studied animals lacking the CLEC2 receptor (27). CLEC2 is expressed predominantly on platelets and its activation by PODOPLANIN expressed on the surface of lymphatic but not blood endothelial cells is required to maintain separation of the venous and lymphatic vasculature through formation of a platelet plug at the lympho-venous junction (13, 27, 28). In the absence of CLEC2, there is chronic retrograde flow of blood from the higher pressure venous system into the thoracic duct that impairs forward lymph flow (29). Given the close

physical proximity of the lympho-venous junction to the site at which the pulmonary lymphatic vasculature drains into the thoracic duct, we hypothesized that lymph flow in pulmonary lymphatic vessels in *Clec2*-mutant mice would be significantly compromised. As previously observed in mesenteric lymphatics (29), loss of CLEC2 resulted in dilated and tortuous pulmonary lymphatic vessels (visualized using the *Prox1-EGFP* transgene and immunostaining for VEGFR3) compared to controls by 4 weeks of age (Figure 2A-F). We have previously found that impaired lymph flow due to loss of CLEC2 is associated with abnormal mesenteric collecting lymphatic vessel remodeling characterized by increased and aberrant smooth muscle cell recruitment (29). Consistent with prior observations in the mesentery, increased smooth muscle cell coverage was observed on pulmonary lymphatics in 4-8 week old $Clec2^{-/-}$ mice but not on pulmonary lymphatics in control animals (Figure 2G-I).

Since constitutive CLEC2 deficiency may lead to altered lymphatics due to loss of flow-dependent lymphatic vessel remodeling such as valve formation, as well as impaired lymph node development (29, 30), we next assessed pulmonary lymphatic function in mature mice (aged 8-10 weeks) in which a conditional *Clec2* allele (31) was inducibly deleted following tamoxifen administration using a $Rosa26Cre^{ERT2}$ driver ($Clec2^{fl/fl};Rosa26Cre^{ERT2}$, hereafter referred to has iClec2 KO). As observed in $Clec2^{-/-}$ animals, iClec2 KO mice exhibit reduced lymph flow due to loss of lymph-venous hemostasis and retrograde filling of the lymphatic network with blood that impairs forward lymph flow (13). To measure pulmonary lymphatic flow, AlexaFluor568-labelled dextran was administered intra-tracheally and subsequently detected in the mediastinal lymph nodes that drain the pulmonary lymphatics (32, 33). Drainage of AlexaFluor568-dextran to mediastinal lymph nodes was significantly decreased in iClec2 KO animals, assessed by both visual examination of the lymph nodes using fluorescent microscopy (Figure 2J, K) and by quantification of lymph node fluorescence (Figure 2L), consistent with impaired pulmonary lymphatic function. Since $Clec2^{-/-}$ animals and iClec2 KO animals share a

common lymph-venous pathology, these studies suggest that the findings in the *Clec2*$^{-/-}$ animals described above arise due to loss of lymphatic flow. However, since lymphatic valve development requires lymph flow, the observation that pulmonary lymphatics in *Clec2*$^{-/-}$ mice have valves (Figure 2B,C) indicates some residual lymph flow in these animals (29).

CLEC2 deficiency results in formation of tertiary lymphoid organs in the lung

In addition to drainage of extracellular fluid, lymphatics serve as conduits for immune cell migration from the lungs to draining lymph nodes, where responses to infection and inflammation are coordinated (34, 35). By 4 weeks after birth, peribronchovascular infiltrates were observed in the lungs of *Clec2*$^{-/-}$ mice but not in the lungs of control littermates (Figure 3A-C). These infiltrates arose in close physical proximity to the dilated pulmonary lymphatic vessels in *Clec2*$^{-/-}$ lungs (Figure 3D,E) and were not observed in littermate control lungs at any time point (Figure 3M). Flow cytometry and immunohistochemistry of lung tissue from 8-12 week old *Clec2*$^{-/-}$ mice revealed a significant increase in the number CD11c^{+}CD103^{+} dendritic cells as well as B220^{+} B cells compared to control lungs (Figure 3I,J). An increase in CD3^{+} T cells was also observed in *Clec2*$^{-/-}$ lungs (Supplemental Figure 3). The cellular organization and location of these inflammatory infiltrates was typical of tertiary lymphoid organs (TLOs). TLOs, also known as bronchus-associated lymphoid tissue (iBALT), form in response to chronic inflammation (10, 36). TLOs resemble secondary lymphoid tissue in their organization, and a hallmark of TLOs is the presence of high endothelial venules (HEVs), specialized blood vessels that are found exclusively in lymphoid tissue that enable homing of leukocytes to that site from the blood (9, 10). Consistent with their identification as TLOs, the inflammatory infiltrates in 8-12 week old *Clec2*$^{-/-}$ lungs were organized around cells expressing peripheral lymph node addressin (PNAd, Figure 3K,L), a specific marker of high endothelial venule endothelium (37). Importantly, TLO formation was not detected in other tissues in *Clec2*$^{-/-}$ mice at baseline, even in organs such as the gut that experience a loss of forward lymphatic flow to an equal or greater extent as that

observed in the lungs (29) (Supplemental Figure 4). Whether TLO formation occurs in other organs in *Clec2*$^{-/-}$ mice in response to infection or inflammation is not known.

The observation that TLOs form in proximity to dilated lymphatic vessels in CLEC2-deficient animals suggested that they arise due to impaired lymphatic function. However, since CLEC2 is also expressed on dendritic cells and is required for dendritic cell migration and lymph node development (30, 38), it is possible that TLO formation reflects a requirement for CLEC2 in dendritic cells or other leukocytes rather than a loss of forward lymph flow. To address this possibility, we examined the lungs of mice with platelet-specific loss of CLEC2 (*Clec2*$^{fl/-}$*;PF4Cre*, hereafter referred to as plt-Clec2 KO), that exhibit impaired lymphatic flow due to loss of lympho-venous hemostasis but retain dendritic cell expression of CLEC2 and have normal lymph node development (29). As in *Clec2*$^{-/-}$ mice, pulmonary lymphatics in plt-Clec2 KO animals were dilated and displayed abnormal smooth muscle cell coverage (Figure 4A-F). Plt-Clec2 KO mice also developed TLOs in the lungs with histologic features that were indistinguishable from those observed in *Clec2*$^{-/-}$ mice, including proximity to lymphatic vessels, large numbers of B cells, and the presence of PNAd^{+} HEVs (Figure 4G-O). Flow cytometry of lung tissue from plt-Clec2 KO mice revealed an increase in CD11c^{+} leukocytes compared to control lungs (Figure 4P), similar to what was seen in *Clec2*$^{-/-}$ mice. While TLOs were exceedingly rare in control lungs (Figure 4 and Supplemental Figure 5), they were found throughout the lungs of 8-12 week old plt-Clec2 KO mice (Figure 4Q). These findings support the conclusion that impaired lymph flow is sufficient to cause TLO formation in the lungs.

CLEC2-deficient mice exhibit defects in the drainage of fluid and cells from the lung

We have previously shown that lymphatic drainage of interstitial fluid is required to increase lung compliance prior to birth, thereby enabling successful neonatal lung inflation (2). In contrast, a classic model originally proposed by Ernest Starling maintains that in the mature lung, fluid balance is maintained by opposing osmotic and hydrostatic pressures in blood

capillaries and surrounding tissue (39, 40). In this model, forces that would move fluid from the blood into the interstitium (i.e. positive capillary blood pressure, positive osmotic pressure of interstitial fluid, and negative interstitial pressure in the lung) are precisely balanced by those that would move fluid from the interstitium into the blood (i.e. positive blood osmotic pressure), leaving little role for lymphatic function. Indeed, some large animal physiologic studies have revealed a relatively minor role for pulmonary lymphatics in clearing lung fluid, even in conditions of pulmonary edema (3, 41, 42), although invasive lymphatic flow measurements have documented increased lymphatic flow rates in settings of chronic edema (43, 44). Thus, whether and to what extent lung lymphatics are required to prevent pulmonary edema in the mature lung is not established. We did not find any increase in pulmonary edema in plt-Clec2 KO mice at baseline using wet-to-dry ratio (Figure 5A), consistent with the lack of histologic changes indicative of edema in the lungs of plt-Clec2 KO mice (Figure 4H,I and data not shown). In contrast, plt-Clec2 KO but not control mice exhibited significant pulmonary edema after acid-induced lung injury (Figure 5A).

The accumulation of leukocytes and TLO formation in mice with reduced lymphatic function due to CLEC2 deficiency suggested that a primary function of pulmonary lymphatics is to transport immune cells from the lungs to the draining mediastinal lymph nodes. Migration of leukocytes from the lungs to lymph nodes after infection is essential for the adaptive immune response (34, 45). However, the fact that TLO formation was observed in the lungs of CLEC2-deficient mice in the absence of infection suggested that lymphatic function may be required for leukocyte trafficking from the lung even under healthy conditions. To measure trafficking, leukocytes labelled with cell trace violet (CTV) were administered to mice intra-tracheally and subsequently detected by flow cytometry in the lungs and draining mediastinal lymph nodes of control and iClec2 KO mice at least 4 weeks after tamoxifen treatment (45) (Figure 5B,C), a time point previously found to be associated with impaired pulmonary lymphatic flow (Figure 2J-L). Migration of CTV-labelled leukocytes from the airways to mediastinal lymph nodes via

lymphatics was significantly decreased in iClec2 KO mice (Figure 5D,E). Consistent with this finding, increased numbers of leukocytes were detected following bronchoalveolar lavage of plt-Clec2 KO mice compared to control animals (Supplemental Figure 6). In contrast, movement of leukocytes to mediastinal lymph nodes following intravenous administration was not affected in iClec2 KO mice (Figure 5F). These findings suggest that TLO formation in CLEC2-deficient mice results from accumulation of immune cells in the lungs due to loss of pulmonary lymphatic function that is required for immune cell egress under basal conditions.

Lung-specific lymphatic ablation results in rapid TLO formation in the lung parenchyma

The studies using CLEC2-deficient animals described above suggested that loss of lymphatic vascular function results in TLO formation specifically in the lungs. However, because lymphatic flow is systemically impaired in CLEC2-deficient animals, it is possible that TLO formation resulted from global changes in immune cell activation and/or migration rather than a lung-specific requirement for lymph flow. Furthermore, we could not rule out the possibility that TLOs formed in the lungs of CLEC2-deficient mice due to contact with blood rather than as a consequence of impaired lymphatic flow. To more precisely test the role lymphatic vascular function in the lungs, and to rule out any unexpected secondary effects from blood-filled lymphatics in CLEC2-deficient models, we sought to generate mice in which lymphatic function could be specifically ablated in the adult lung. To accomplish this, mice expressing both Cre-inducible diphtheria toxin receptor (DTR) (46) and tamoxifen-inducible Cre recombinase driven by the lymphatic-specific VEGFR3 promoter (47) (*iDTR;VEGFR3Cre*^{ERT2}) were used as donors for lung transplantation (Figure 6A). VEGFR3 expression is restricted to lymphatic endothelial cells in the mature lung, and lineage tracing confirmed that the *VEGFR3Cre*^{ERT2} transgene is active specifically in those cells (Supplemental Figure 7). Tamoxifen administration to *iDTR;VEGFR3Cre*^{ERT2} mice induces expression of DTR in lymphatic endothelial cells of the donor lungs, rendering all lymphatic endothelial cells in the lung susceptible to cell death

following exposure to diphtheria toxin A (DT). The left lungs from donor *iDTR;VEGFR3Cre^{ERT2}* mice were transplanted into control littermates. Although lymphatic vessels were not surgically reconnected after lung transplant, studies in mice and large animals have demonstrated that lymphatic drainage is reestablished 7-21 days after transplantation (33, 48, 49). DT was administered 21 days after transplantation of the *iDTR;VEGFR3Cre^{ERT2}* lung to ensure that lymphatics function was first reestablished in the transplanted lungs (Figure 6A). Rejection of the transplanted lung was prevented by back-crossing to C57Bl/6 background and by the strict use of littermates for donor and recipient animals.

Immunostaining of the *iDTR;VEGFR3Cre^{ERT2}* lung isografts for the lymphatic endothelial markers LYVE1 and PROX1 5 days after onset of DTA administration revealed a greater than 50% loss of lymphatic endothelial cells compared to control transplanted lungs (Figure 6B-D), a finding predicted to impair lymphatic function. We did not observe any significant amount of blood in the lymphatics of control transplanted lungs or in the remaining lymphatics in transplants with DT-mediated lymphatic deletion (Supplemental Table 2), confirming that this model does not result in retrograde blood flow into the lymphatic vessels as seen in CLEC2-deficient mice. Significantly, abundant TLO formation, marked by the presence of large numbers of B220$^+$ cells and PNAd$^+$ HEVs, was observed in *iDTR;VEGFR3Cre^{ERT2}* transplanted lungs that were treated with DT but not in control transplanted lungs with intact lymphatics (Figure 6E). Strong correlation between the extent of lymphatic endothelial cell loss and the formation of TLOs was observed, as greater numbers of TLOs were detected in transplanted lungs that exhibited greater deletion of lymphatic endothelial cells (Figure 6F). The TLOs that formed after lymphatic deletion closely resembled those in the lungs of plt-Clec2 KO mice in their location, appearance, and cellular composition (Figure 7A-P). The rapidity with which TLOs formed after lymphatic deletion in this model (within 5 days) compared to those in CLEC2-deficient mice (at least 4 weeks) was notable. This likely reflects the effects of acute and severe disruption of lymphatic flow in this model, as opposed to the more mild and chronic impairment of lymphatic

flow conferred by loss of CLEC2. These results provide a second line of genetic evidence to support the conclusion that loss of lymphatic function in the lung results in TLO formation.

Constitutive loss of CLEC2 results in an emphysematous lung phenotype

TLO formation is commonly seen in chronic lung inflammation and is associated with diverse lung diseases in humans (10, 36), but whether TLO formation is connected to impaired lymphatic flow, and whether TLOs are a cause or a consequence of lung disease remains unclear (50, 51). The primary formation of TLOs in mice with impaired lymphatic flow allowed us to ask whether lymphatic impairment might lead to lung injury and pathology. Although TLOs formed as early as P35 in plt-Clec2 KO mice, we did not observe any significant lung parenchymal changes at this time point (Supplemental Figure 8). However, 6-8 month old plt-Clec2 KO mice exhibited marked alveolar enlargement similar to that observed in the human lung disease emphysema (Figure 8A-C). This was not due to a primary defect in alveolarization in these mice, as there was no appreciable alveolar enlargement prior to P36 (Supplemental Figure 8), a time point by which alveolar development is nearly complete (52). The emphysematous alveolar phenotype in plt-Clec2 KO mice was associated with hypoxia, an indicator of significant impairment of lung function (Figure 8D). A hallmark of human emphysema is the breakdown of elastin in the alveolar walls due to secretion of degrading proteases by macrophages and neutrophils (53, 54). Immunostaining revealed reduced elastin in lungs from plt-Clec2 KO mice compared to control littermates, particularly in areas where the emphysema phenotype was most pronounced (Figure 8E,F). Severe emphysema in humans is associated with the generation of elastin fragments which are considered a marker of active disease (55) and may drive disease progression (56-58). A significant increase in a 25kD elastin fragment and a nonsignificant increase in a 45kD elastin fragment was detected in the lungs of 6-8 month old plt-Clec2 KO mice compared to control animals (Figure 8G,H and Supplemental Figure 9). Expression of the elastin-degrading matrix mettaloproteinase-12 (MMP-12) is

required for the development of cigarette smoke-induced emphysema in mice and is upregulated in humans with this disease (53, 59, 60). Increased MMP-12 was detected in the lungs of mice with loss of CLEC2 by both qPCR and immunohistochemistry (Figure 8I-K). Since the only described effect of CLEC2-deficiency on the lung is impaired lymphatic flow, these results suggest that chronic loss of lymphatic function is sufficient to confer a lung phenotype with molecular and cellular features of emphysema.

Discussion

Organ-specific roles have recently emerged as a central mechanism by which the vascular system functions in both healthy and diseased states (61), but designing studies to identify these roles in the lymphatic system is challenging due to the lack of organ-specific lymphatic markers and tools to target the lymphatic vasculature of a particular organ. The present studies identify unique anatomic and functional features of pulmonary lymphatic vessels. The finding that lymphatic vessels lack smooth muscle cell coverage is unique to the lung and suggests that pulmonary lymph flow is maintained by other mechanisms, e.g. respiratory movements and changes in thoracic pressure. The inability of lung collecting lymphatics to independently pump lymph may make these vessels uniquely susceptible to blockage and dysfunction. Consistent with this idea, we observed that following global impairment of lymphatic function, spontaneous formation of TLOs occurs specifically in the lung. We propose that these unique anatomical and functional features are connected, and that they may link changes in lymphatic vessel function to the pathogenesis of common lung diseases.

In the present study, we used two distinct approaches to examine loss of pulmonary lymphatic function in the mouse: genetic deletion of CLEC2, a platelet receptor required to maintain forward pulmonary lymph flow, and the transplantation of lungs genetically engineered to allow inducible ablation of lymphatic endothelial cells. The findings using these two models are highly concordant, and demonstrate a lung-specific role for lymphatic vessels in preventing a chronic inflammatory state characterized by the formation of TLOs. We also find that chronically impaired lymphatic flow due to loss of CLEC2 results in alveolar enlargement and hypoxia with features of lung injury that resemble emphysema. These findings establish an organ-specific role for lymphatic vessels in the lung, and suggest that impairment of lung lymphatic function may participate in the pathogenesis of lung diseases such as emphysema that are associated with TLO formation.

An established, and often considered universal, role of lymphatic vessels is to take up interstitial fluid and proteins that leak from the blood vasculature, thereby preventing tissue edema. Consistent with this role, a hallmark sign of generalized loss of lymphatic function is tissue edema (62), and lymphatic function is required for fluid drainage in the developing lung to enable neonatal lung inflation (2). Although large animal studies using short-term catheter-based approaches have demonstrated that lymphatic flow in the lung may be dynamic (21, 22) pulmonary edema can also be considered a consequence of imbalanced Starling forces in the alveolar blood capillary rather loss of lung lymphatic function (63). Our studies of CLEC2-deficient lungs provide a first genetic insight into the long-term role of lymphatic vessels in the management of fluid homeostasis in the mature lung. Lung wet-to-dry ratios were not elevated in CLEC2-deficient lungs at baseline. Though this is an insensitive measure of pulmonary edema, the absence of histologically apparent edema in the lungs of CLEC2-deficient mice suggests that any pulmonary edema that results from impaired lymphatic drainage is unlikely to be severe in the otherwise healthy lung. However, we did observe increased wet-to-dry ratio in response to lung injury in CLEC2-deficient mice, indicating that lymphatic dysfunction does contribute to pulmonary edema in this setting and establishing a role for pulmonary lymphatics in lung fluid management. Future studies addressing pulmonary lymphatic function in other pathologic settings are likely to shed additional light on this role.

The most prominent effect of impaired pulmonary lymphatic function observed in these studies was the formation of TLOs, a pathology detected following both loss of CLEC2 and LEC ablation in transplanted lungs. Since these in vivo models share no molecular or cellular features other than loss of lymphatic function, this phenotype is highly likely to be a specific consequence of lymphatic impairment. This conclusion is also supported by the fact that TLOs were observed adjacent to collecting lymphatic vessels. Moreover, although CLEC2-deficient mice experience loss of mesenteric and intestine lymphatic function that is similar in magnitude to that in the lung (29), TLOs are selectively observed in the lungs of CLEC2-deficient mice.

Why does loss of lymphatic function result in TLO formation specifically in the lung? One possible explanation for this organ specificity is that pulmonary lymphatic vessels transport a larger number of immune cells than lymphatic vessels in other organs due to the fact that the lung is a barrier organ exposed to the outside environment. An alternative explanation is suggested by the unique anatomy of pulmonary lymphatic collecting vessels that lack virtually all SMC coverage. The lack of SMC coverage may make pulmonary collecting lymphatics more permeable than those in other organs and facilitate cellular extravasation when lymph flow is impeded (e.g. the CLEC2 KO model) or when the lymphatic endothelial barrier is disrupted (e.g. the LEC ablation model). In either case, the fact that lymphatic impairment is sufficient to confer TLO formation in an otherwise healthy lung suggests that changes in lymphatic function may play an important role in lung pathology.

TLO formation is a common histologic feature of chronic lung inflammation that is observed in emphysema, lung transplant rejection, and pulmonary complications of rheumatoid arthritis (64-66). However, whether TLO formation is a cause or consequence of these disease processes has not been clear. In CLEC2-deficient mice, TLO formation in the lung is an early event that is followed by evidence of lung injury characterized by alveolar enlargement, breakdown of tissue elastin, and significant hypoxia - all features of cigarette smoke-induced emphysema in humans. The clear temporal sequence of these events, and the fact that platelet CLEC2 deficiency appears to only impact the lung indirectly through changes in lymph flow, suggest that TLO formation may be a causal mechanism in lung injury, and that lymphatic dysfunction may underlie both TLO formation and lung disease pathogenesis. The fact that abnormal lymphatic vessels have been observed in a variety of chronic lung diseases (12) provides additional evidence for considering this possibility. Future studies will address the precise role of lymphatic function in the pathogenesis of common lung diseases associated with TLO formation, and how cigarette smoke exposure may directly affect lymphatic vessel function.

Methods

Animal models

Clec2^{-}, *Clec2*^{fl}, *PF4-Cre*, and *Prox1-EGFP* BAC transgenic mice have been previously described by our lab (23, 29) and were maintained on a mixed background. *Rosa26-iDTR* and *Rosa26-iYFP* mice were purchased from Jackson Laboratory. *VEGFR3Cre*^{ERT2} mice (a gift from Sagrario Ortega) have been previously described (47). For transplant experiments, all mice were maintained on C57Bl/6 background. For all experiments, both male and female mice were used.

Whole mount staining

Tissue from mice carrying the *Prox1-EGFP* transgene was fixed overnight in 4% PFA at 4^{o}C. For lungs, thick coronal sections were made using a scalpel. Other tissues were stained intact. Tissue was permeabilized in 0.1% BSA + 0.3% Triton-X in PBS. Incubation with Cy3-conjugated anti-smooth muscle actin antibody (Sigma, C6198) was performed in 0.3% Triton-X in PBS. The tissue was imaged using a Leica TCS SP8 confocal microscope.

Dextran Assay

50ul of 5mg/ml dextran-568 (10,000kD MW, ThermoFisher) was administered to anesthetized, intubated mice via endotracheal catheter. Fifty minutes after administration, the mice were sacrificed for harvest of mediastinal lymph nodes. This time point is based both on previous reports using this assay (33) and our own studies demonstrating the time course of dextran drainage to the mediastinal lymph nodes after intra-tracheal delivery (Supplemental Figure 2). Lymph nodes were imaged using an Olympus SZX16 dissecting microscope. Quantification of fluorescence intensity was performed using ImageJ.

Immunohistochemistry

Mice were sacrificed and tissue was perfused with PBS. Lungs were inflated with 4% PFA at constant pressure of 25 cm H_2O prior to harvest and fixation with 4% PFA overnight. Slides from paraffin-embedded sections were H&E stained or immunostained with antibodies for: B220 (Abcam, ab 64100), CD3 (Abcam, ab16669), PNAd (BD Biosciences, 553863), Lyve-1 (R&D Systems, AF2125 Systems), VEGFR3 (R&D Systems, AF743), Prox1 (Abcam, ab76696) MMP-12 (Abcam, ab128030), CD31 (HistoBiotec, DIA 310), and NG2 (Millipore, AB5320). Slides of normal human lung tissue was stained with antibodies for PODOPLANIN (D240, Abcam, ab77854). Elastin was detected using Modified Verhoeff Van Gieson Stain Kit (Sigma).

Cell Tracing Assay and Flow Cytometry

Splenocytes were isolated from wild-type mouse spleens and cultured overnight with 100ng/ml LPS and 5ug/ml PHA (Sigma). The cells were then labeled with cell trace violet (CTV, Molecular Probes) according to manufacturer instructions. $1x10^7$ CTV-labeled cells were administered to anesthetized and intubated mice either via endotracheal catheter or intravenously. Lymph nodes or lungs were harvested 48 hours after administration of CTV-labeled cells. Single cell suspensions were stained with the following antibodies: FITC-conjugated anti-CD45 (eBioscience, 11-04551-82), PE-Cy7-conjugated anti-CD11c (BD Bioscience, 561022), and PerCP/Cy5.5-conjugated anti-CD103 (Biolegend, 121415). Flow cytometry was performed using a BD FACSCanto, and analyzed using FlowJo software.

Bronchoalveolar Lavage

Mice were sacrificed and bronchoalveolar lavage (BAL) was then performed through a 20-gauge angiocatheter (BD Pharmingen, San Diego, CA), with the intra-tracheal instillation of 1 ml phosphate-buffered saline (PBS) containing an anti-protease cocktail (Sigma) and 5 mM EDTA given in 0.5 ml increments. Total leukocyte cell count (cells/ml BAL fluid) was measured using a Coulter Cell and Particle Counter (Beckman Coulter, Miami, FL).

Quantitative PCR and Western Blotting

Total RNA was isolated from lung tissue using RNEasy Kit (Qiagen). cDNA was made using Superscript III First-Strand Synthesis System (Invitrogen) following manufacturer instructions. qPCR analysis of gene expression was performed using QuantStudio 6 Real-Time PCR System and SYBR Green PCR Master Mix (Applied Biosystems). Analysis of relative gene expression was carried out using the comparative CT method (ΔCT) using GAPDH as the reference housekeeping gene. Each qPCR reaction was performed in triplicate. Western blots were performed according to standard protocols and probed with anti-elastin (Abcam, ab21610) and anti-beta actin antibodies (Abcam, ab8226). Blots were imaged using LI-COR Imaging Systems and quantified using ImageJ.

Acute Lung Injury

Mice were exposed to acid-induced lung injury as previously described (67). Briefly, 30μl of 0.1N HCl was administered to anesthetized and intubated mice either via endotracheal catheter. Anesthetized mice were ventilated for 1 hour after acid administration, at which time they were euthanized for tissue harvest. Left lungs were weighed immediately after removal (wet weight) and again after drying in an oven at 55°C for 48 hours (dry weight).

Lung Transplants and Pulmonary Lymphatic Ablation

iDTR;VEGFR3CreERT2 mice were used as donors for single lung transplant into control littermates. Expression of the DTR is induced by administering tamoxifen i.p. for five consecutive days prior to transplant. The heart-lung block was harvested and flushed with heparin and saline. The left lung was then isolated. The recipient mouse was anesthetized with isoflurane, intubated, and connected to a ventilator. The mouse was then placed in the supine position and an incision made at the left chest between the 3rd and 4th ribs to expose the left pulmonary artery and vein. After a micro-serrefine clamp (FST 18055) was placed at the left

hilum, transverse incision was made on the left bronchus. A running stitch of 11-0 suture (Ethilon 2881G) was used for end-to-end anastomosis of donor to recipient bronchus. Donor pulmonary artery and vein were connected to recipient pulmonary artery and vein respectively end to side using the same 11-0 suture. The native left lung was removed after implantation of the donor lung. Lymphatic deletion in transplanted lungs was induced 21 days after transplant by administering 5 g of DTA (Sigma) over 72-hours using a subcutaneous pump (Alzet).

Assessment of Oxygen Saturation

Mice were anesthetized using isoflurane, and pulse oximetry was performed using a MouseSTAT (Kent Scientific). For each mouse, oxygen saturation was recorded every 10 seconds for 1 minute, and these values were averaged. Mice were monitored and anesthesia was adjusted to ensure that the heart rate was maintained at greater than 400bpm for all measurements, and oxygen saturation was being consistently detected.

Statistics

Quantification of TLOs in lung tissue was performed using 4X images (1.1 x 1.3mm), with at least 3 images used for each mouse. TLOs were defined as discrete leukocyte-dense accumulations on H&E sections that were predominantly B-cells or had $PNAd^+$ HEVs by immunohistochemistry on serial sections. Quantification of SMA staining on $VEGFR3^+$ lymphatics was done on doubled stained slides of lung tissue from control mice. 30 randomly selected $VEGFR3^+$ lymphatic vessels were imaged at 20X magnification, and each vessel was assessed for any associated SMA staining. Quantification of $Prox1^+Lyve1^+$ endothelial cells was performed by scoring double positive nuclei using 20X images of immunostained tissue from lung transplants. At least 10 randomly selected images were used for each mouse. Quantification of mean linear intercept was performed as previously described (68). Briefly, the sum of the lengths of lines drawn across the images was divided by the number of intersections

between alveolar walls. At least ten 20X images of lung tissue from each mouse were used for analysis. Data shown are expressed as mean ± SEM, and number of samples per condition are indicated in figure legends. Statistical significance was determined by unpaired two-tailed Student's *t* test or ANOVA using Prism statistical software. *P* values less than 0.05 were considered statistically significant.

All animal experiments were approved by The University of Pennsylvania Institutional Animal Care and Use Committee.

Author Contributions

H.O.R. designed and performed experiments and drafted the manuscript. L.W. performed lung transplantation procedures. J.S. provided technical assistance. J.Y assisted with sectioning of slides and immunohistochemistry. M.C. and L.L. performed genotyping and assisted in experiments. P.A. and Z.J. provided tissue samples and assistance with the manuscript. J.D. provided technical assistance and advice on lung phenotypes. W.H provided assistance with lung transplant experiments. M.L.K. oversaw experimental design and writing of manuscript.

Acknowledgements

The authors thank the University of Pennsylvania Histology Core Facility and the University of Pennsylvania Animal Facility (particularly Latrise Bennett) for support. We thank Michael Beers, Yaniv Tomer, Meghan Kopp, and Melpo Christofidou-Solomidou for technical expertise and advice. We thank Kunal Patel and John Wherry for assistance with cell tracing experiments. Human lung tissue was generously provided by the Penn Center for Pulmonary Biology Human Lung Tissue Bank. This work was supported by T32HL007586-32 (to H. Outtz Reed) and by NIH grant R01 HL121650 (to M.L. Kahn).

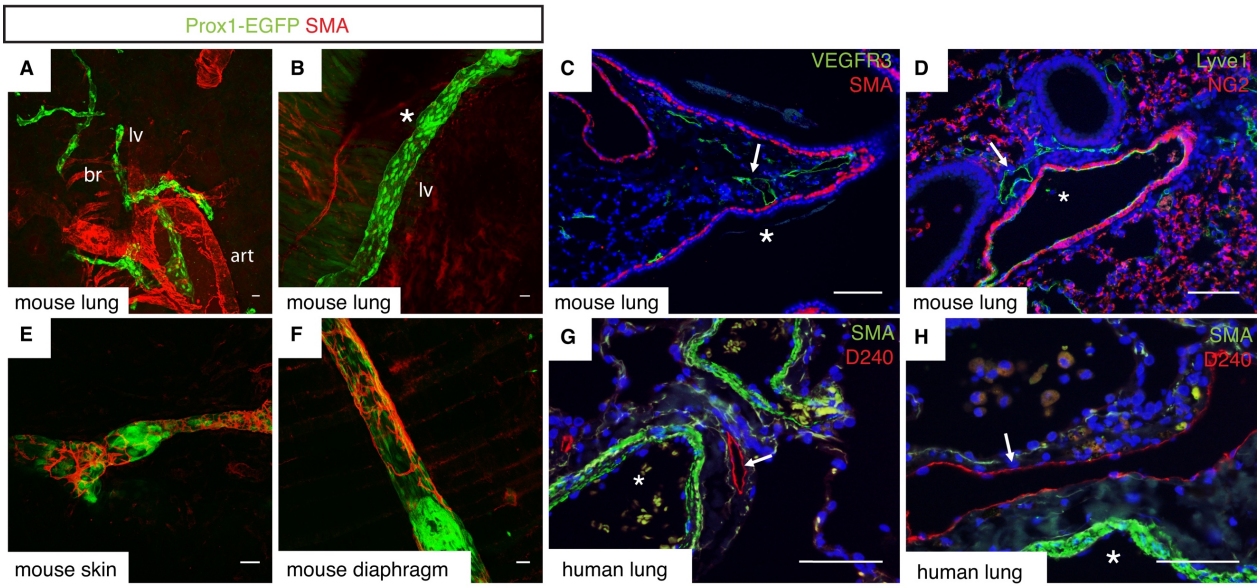

Figure 1: Pulmonary collecting lymphatics lack smooth muscle cell or pericyte coverage. (A,B) Whole mount imaging of lungs from adult *Prox1-EGFP* lymphatic reporter mice shows pulmonary lymphatic vessels (lv) in green, with asterisk indicating an area of Prox1^{hi} endothelial cells that marks lymphatic valves. Note staining for smooth muscle actin (SMA, red) present on both the bronchi (br) and arteries (art). (C,D) Immunohistochemistry of lung sections shows pulmonary lymphatics in green using staining for VEGFR3 or Lyve1 (arrows). Staining for SMA (C, red) or NG2 (D, red) marks airways or blood vessels, respectively. Asterisks indicate the large airway (C) or blood vessel (D) in proximity to lymphatic vessels. (E,F) Whole mount staining for SMA (red) on lymphatic vessels in skin (E) and diaphragm (F) in *Prox1-EGFP* mice. (G,H) Human lung tissue sections were stained for the lymphatic molecular marker PDPN using the D240 antibody (red, arrows) and SMA (green), with arteries indicated by asterisk. Scale bars = 25μm.

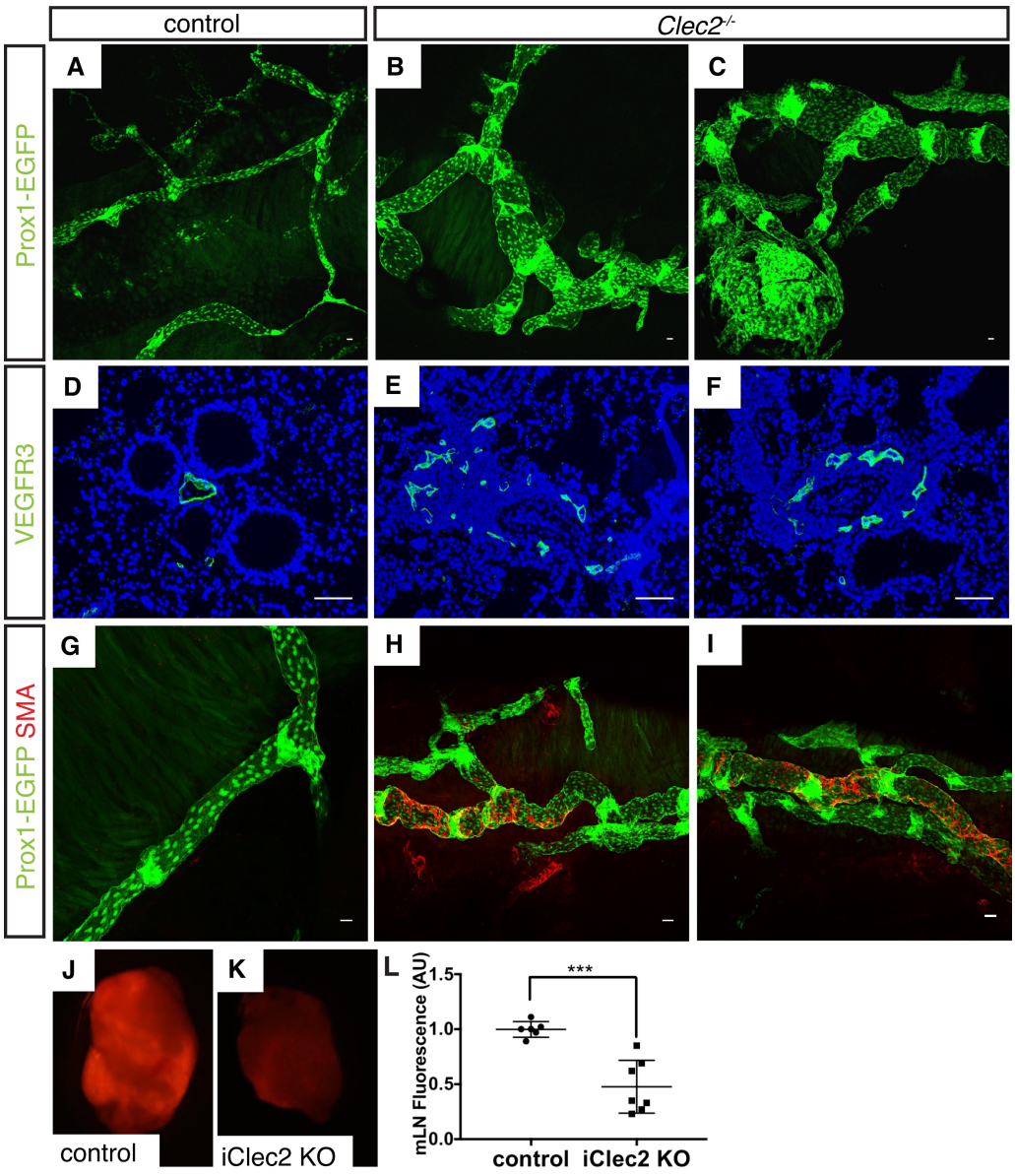

Figure 2: CLEC2-deficient mice exhibit impaired lymphatic flow. (A-C) Whole mount imaging of pulmonary lymphatic vessels (green) using the lymphatic reporter *Prox1-EGFP* in 4-8 week old *Clec2*$^{-/-}$ and control mice is shown. (D-F) Immunohistochemistry of lung sections for VEGFR3 (green) shows lymphatic vessels in 4-8 week old *Clec2*$^{-/-}$ and control mice. (G-I) Whole mount staining of pulmonary lymphatic vessels (*Prox1-EGFP*, green) in 4-8 week-old *Clec2*$^{-/-}$ and control mice for smooth muscle actin (SMA, red). (J,K) Fluorescence microscopy of mediastinal lymph nodes (mLN) from iClec2 KO and control mice 50 minutes after intra-tracheal administration of dextran-568 (red). (L) Quantification of dextran-568 uptake to mediastinal lymph nodes by mean fluorescence intensity (AU). Scale bars = 25μm. Data are representative of at least 5 mice in each group. All values are means ± SEM. *P* value calculated by Student's *t* test. ***$P < 0.001$.

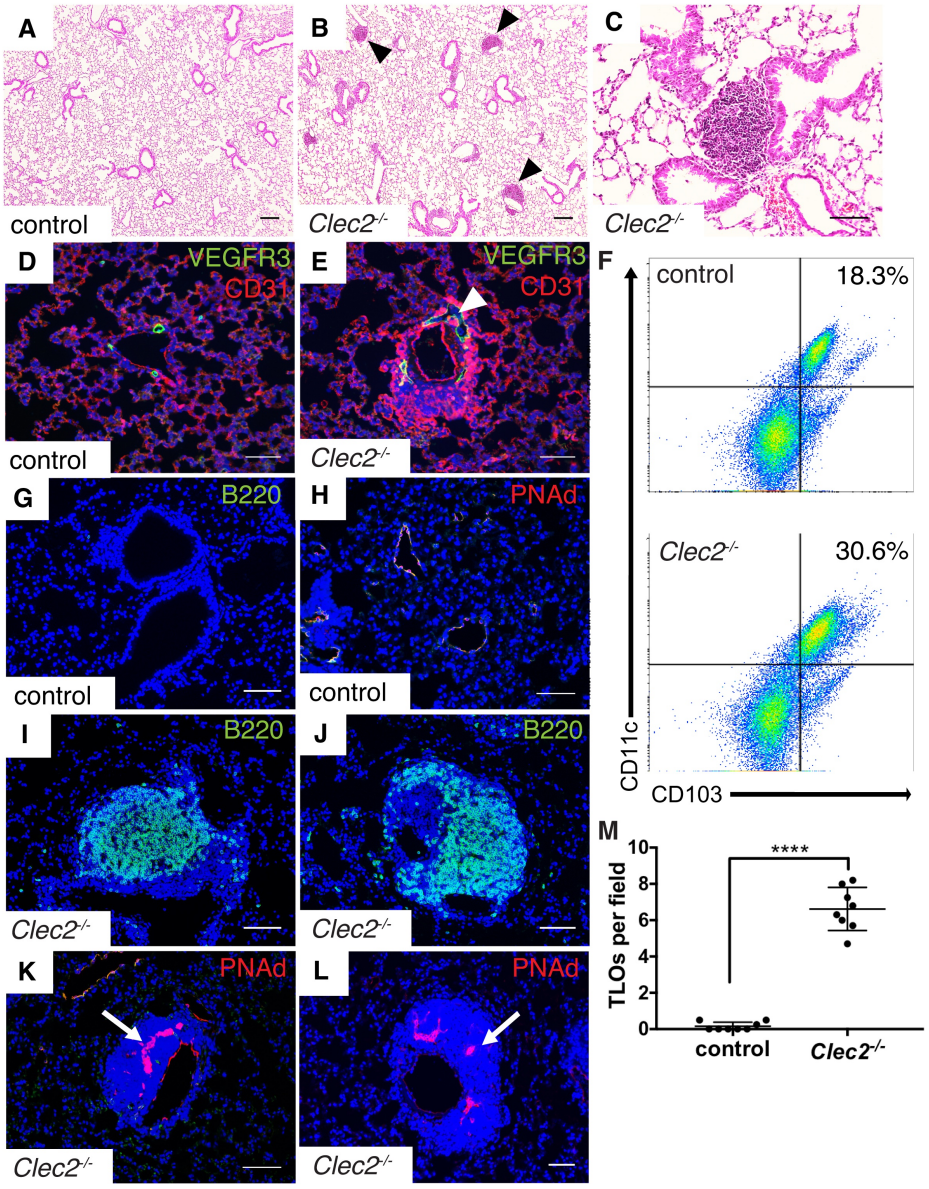

Figure 3: Loss of CLEC2 is associated with abnormal tertiary lymphoid organ (TLO) formation in the lung parenchyma. (A-C) H&E staining of lung tissue from 4-6 week old *Clec2*$^{-/-}$ and control mice. Arrowheads indicate inflammatory infiltrates. (D,E) Staining for pulmonary lymphatic vessels (VEGFR3, green) and capillaries (PECAM, red). Arrowheads indicate dilated pulmonary lymphatic vessels in the lung of a *Clec2*$^{-/-}$ mouse. (F) Flow cytometry of lung tissue from 8-12 week old control (top) and *Clec2*$^{-/-}$ mice (bottom) for CD103^{+} CD11c^{+} cells. Samples were gated for CD45^{+} leukocytes. (G-L) Immunohistochemistry for B cells (B220, green) and high endothelial venules (PNAd, red, arrows) in *Clec2*$^{-/-}$ and control mice. (M) Quantification of TLOs in the lungs of 8-12 week old *Clec2*$^{-/-}$ mice compared to control littermates per 4x (1.1 x 1.3mm) microscopic field. Data representative of at least 5 mice in each group. Scale bars in A and B = 100μm. All other scale bars = 25μm. All values are means ± SEM. *P* value calculated by Student's *t* test. **** *P* <0.0001.

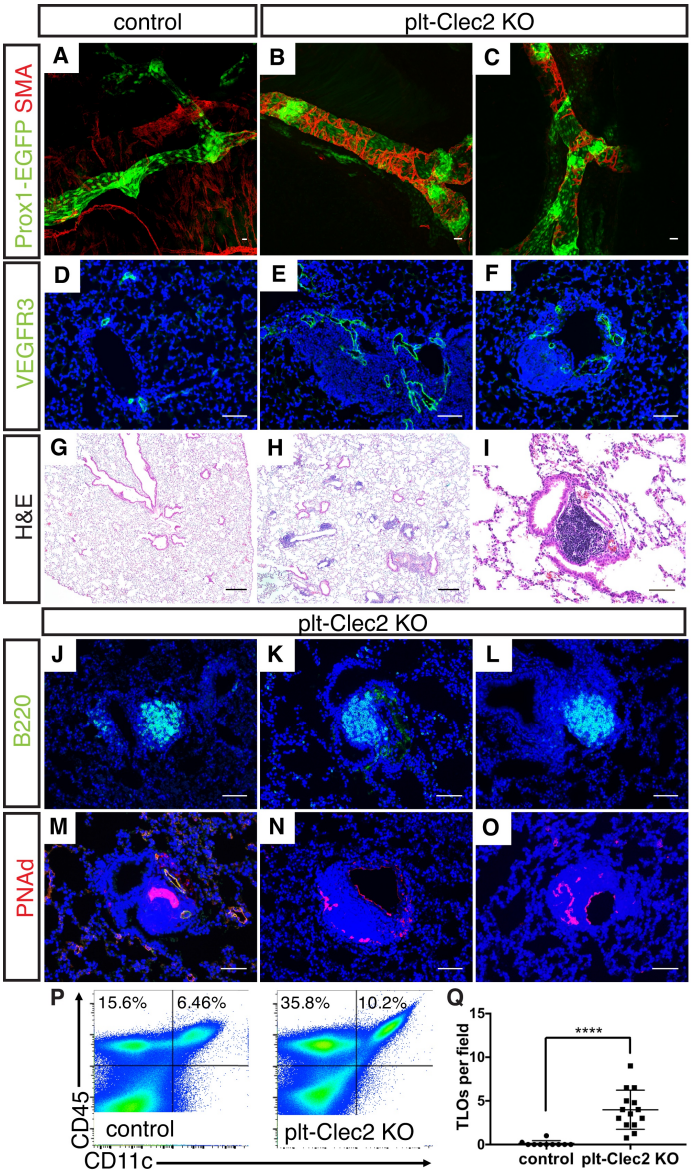

Figure 4: Platelet-specific loss of CLEC2 results in abnormal pulmonary lymphatic morphology and TLO formation in the lung parenchyma. (A-C) Whole mount staining of pulmonary lymphatic vessels (*Prox1-EGFP*, green) in 6-8 week-old plt-Clec2 KO and control mice for smooth muscle actin (SMA, red). (D-F) Immunohistochemistry of sections from lung tissue for VEGFR3 (green) shows lymphatic vessels in 6-8 week old plt-Clec2 KO and control mice. (G-I) H&E staining of lung tissue from 8-12 week old plt-Clec2 KO and control mice. (J-O) Immunohistochemistry for B cells (B220, green) and high endothelial venules (PNAd, red) in plt-Clec2 KO and control mice. (P) Flow cytometry of lung tissue from control (left) and plt-Clec2 KO mice (right) for $CD45^+$ $CD11c^+$ cells. (Q) Quantification of TLOs in the lungs of 8-12 week old plt-Clec2 KO mice compared to control littermates per 4x (1.1 x 1.3mm) microscopic field. Data representative of at least 5 mice in each group. Scale bar in G and H = 100μm. All other scale bars = 25μm. All values are means ± SEM. *P* value calculated by Student's *t* test. **** *P* <0.0001.

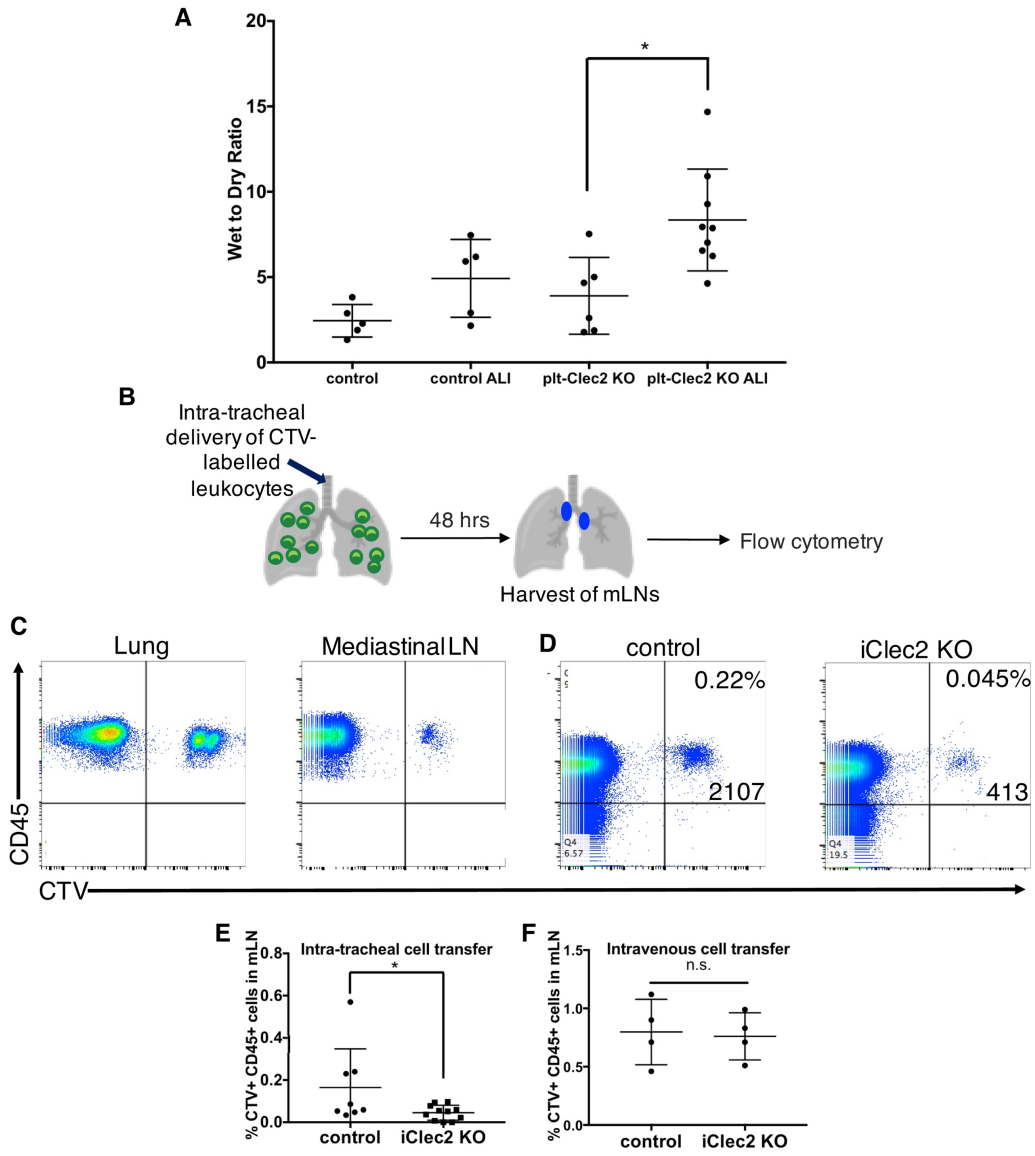

Figure 5: Loss of CLEC2 results in impaired drainage of fluid and cells from the lung. (A) Wet-to-dry ratios of control and plt-Clec2 KO lungs at baseline and in response to acid-induced lung injury (ALI). (B) Cell tracing experiment to assess lymphatic leukocyte trafficking from lungs to draining lymph nodes. Intra-tracheal administration of CTV-labeled leukocytes is followed by harvest of mediastinal lymph nodes (mLN) for flow cytometry. (C) Identification of $CD45^+$ CTV^+ leukocytes in the lungs (left) and mediastinal lymph nodes (right) 48 hours after intra-tracheal administration in wild-type mice. (D) Flow cytometry of mLN from iClec2 KO (right) and control (left) mice for $CD45^+$ CTV^+ leukocytes 48 hours after intra-tracheal administration. (E) Quantification of CTV^+ leukocytes in control and iClec2 KO mLNs after intra-tracheal administration, as percent of total $CD45^+$ leukocytes. (F) Quantification of CTV^+ leukocytes in control and iClec2 KO mLNs after intravenous administration as percent of total $CD45^+$ leukocytes. Data representative of at least 4 mice in each group. All values are means ± SEM. *P* value calculated by Student's *t* test. * $P < 0.05$. n.s. = not significant.

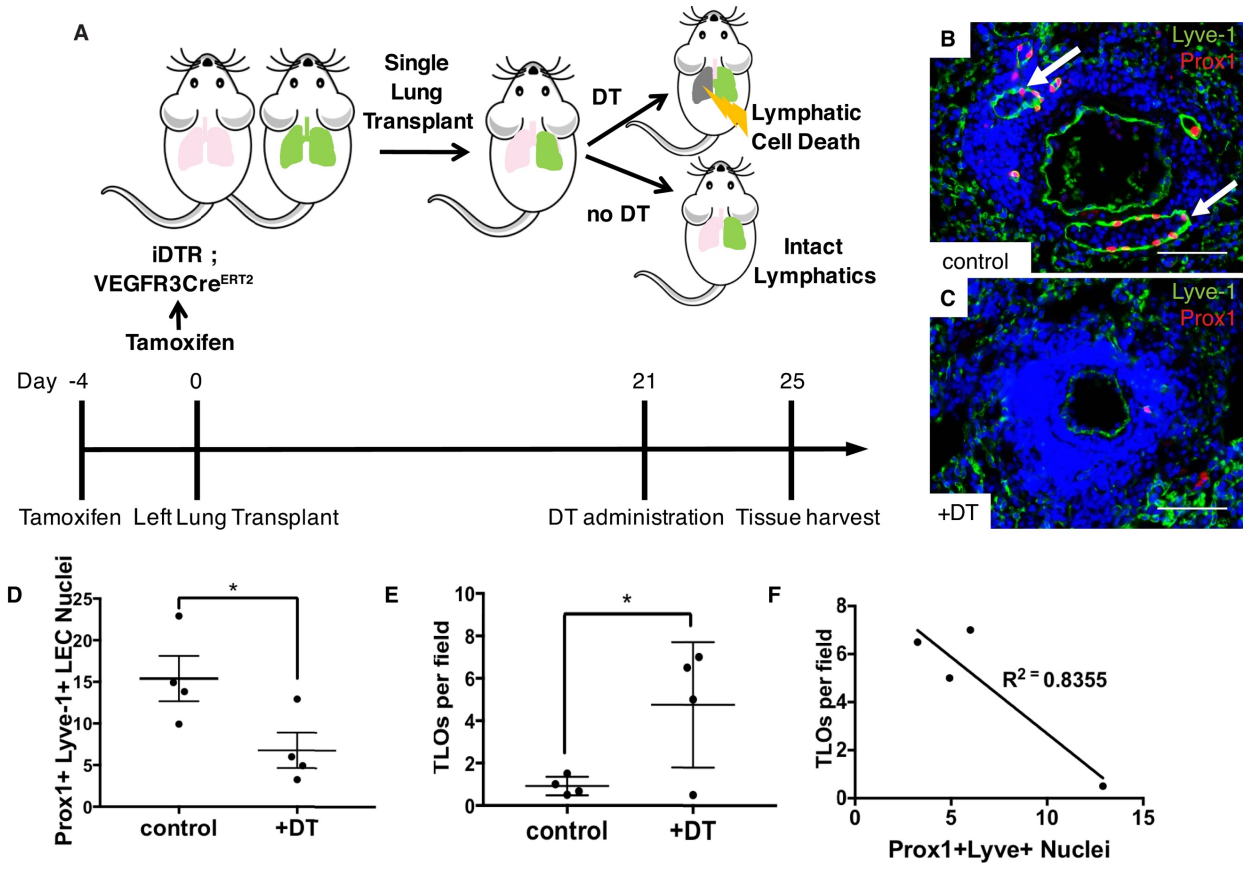

Figure 6: Lung-specific lymphatic endothelial cell ablation leads to TLO formation. (A) Top: Schematic of the experimental approach used for lung-specific deletion of pulmonary lymphatics. Diphtheria toxin receptor (*iDTR*) expression is induced in lymphatic endothelial cells using a lymphatic endothelial cell-specific Cre (*VEGFR3Cre^{ERT2}*). Lungs from *iDTR;VEGFR3Cre^{ERT2}* mice are used as donors for single lung transplant to littermate recipients, and administration of DT to transplanted mice leads to lymphatic endothelial cell death specifically in the transplanted lung, while control transplanted lungs have intact lymphatics. Bottom: Timeline of lung-specific lymphatic ablation in lung transplants. (B,C) Immunohistochemistry for Prox1^{+}Lyve-1^{+} lymphatic endothelial cell (LEC) nuclei in control lungs (B, arrows) and lungs with DT-mediated lymphatic ablation (C). (D) Quantification of Prox1^{+}Lyve-1^{+} nuclei in DT-treated *iDTR;VEGFR3Cre^{ERT2}* transplanted lungs compared to control transplanted lungs. (E) Quantification of TLOs in DT-treated *iDTR;VEGFR3Cre^{ERT2}* transplanted lungs compared to control transplants per 4x (1.1 x 1.3mm) microscopic field. (F) Correlation of TLOs to number of Prox1^{+}Lyve^{+} LEC nuclei in DT-treated *iDTR;VEGFR3Cre^{ERT2}* transplanted lungs. Data representative of 4 mice in each group. Scale bars = 25μm. All values are means ± SEM. * *P* <0.05. *P* value calculated by Student's *t* test.

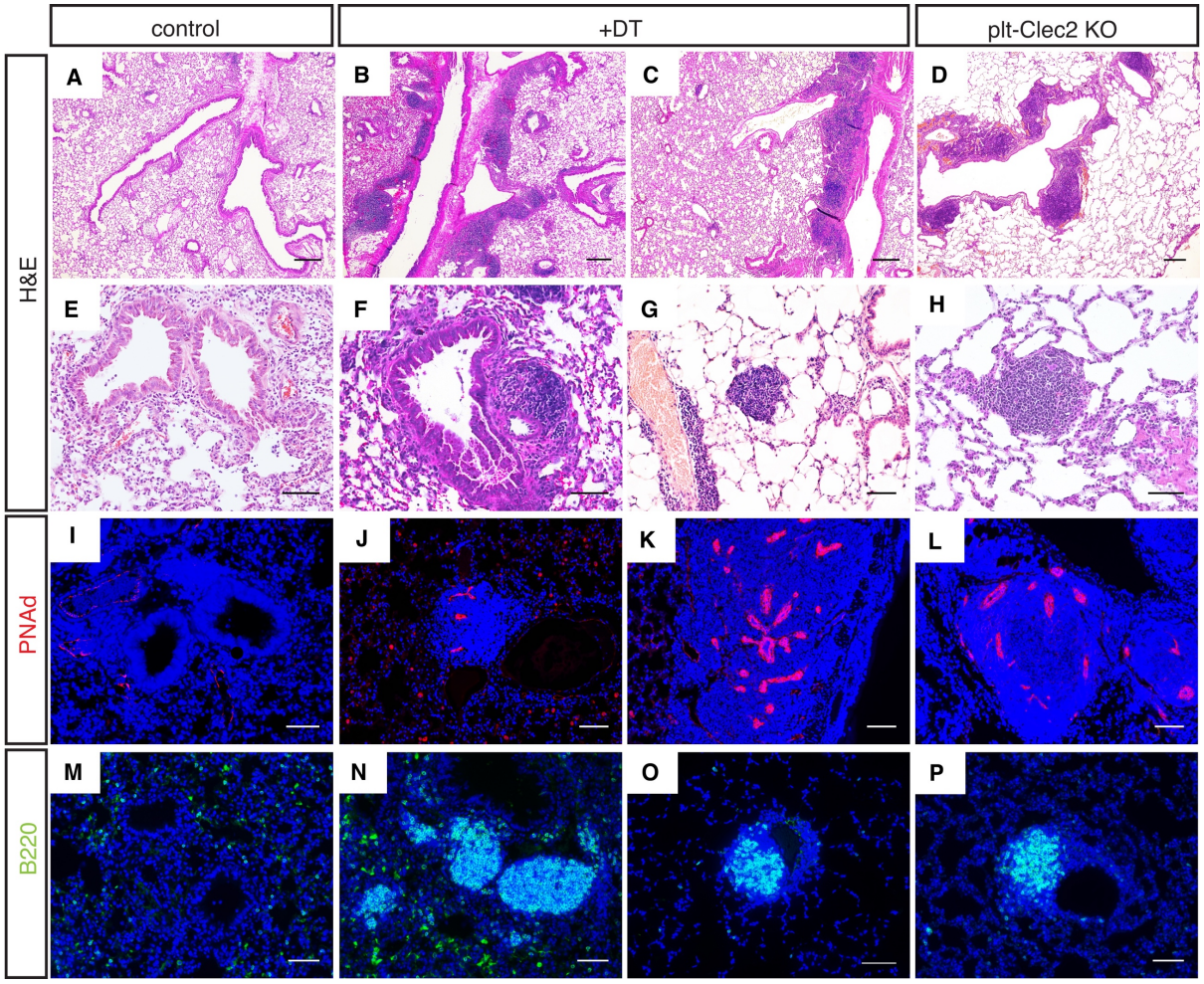

Figure 7: TLOs after lung lymphatic ablation resemble those in plt-Clec2 KO mice. (A-H) H&E staining of lung tissue from control transplanted lungs, DT-treated *iDTR;VEGFR3Cre*^{ERT2} transplanted lungs with lymphatic ablation, and lungs from plt-Clec2 KO mice. (I-P) Immunohistochemistry for B cells (B220, green) and HEVs (PNAd, red) in control transplanted lungs, DT-treated *iDTR;VEGFR3Cre*^{ERT2} transplanted lungs, and plt-Clec2 KO lungs. Data representative of 4 mice in each group. Scale bars in A-D = 100μm. All other scale bars = 25μm.

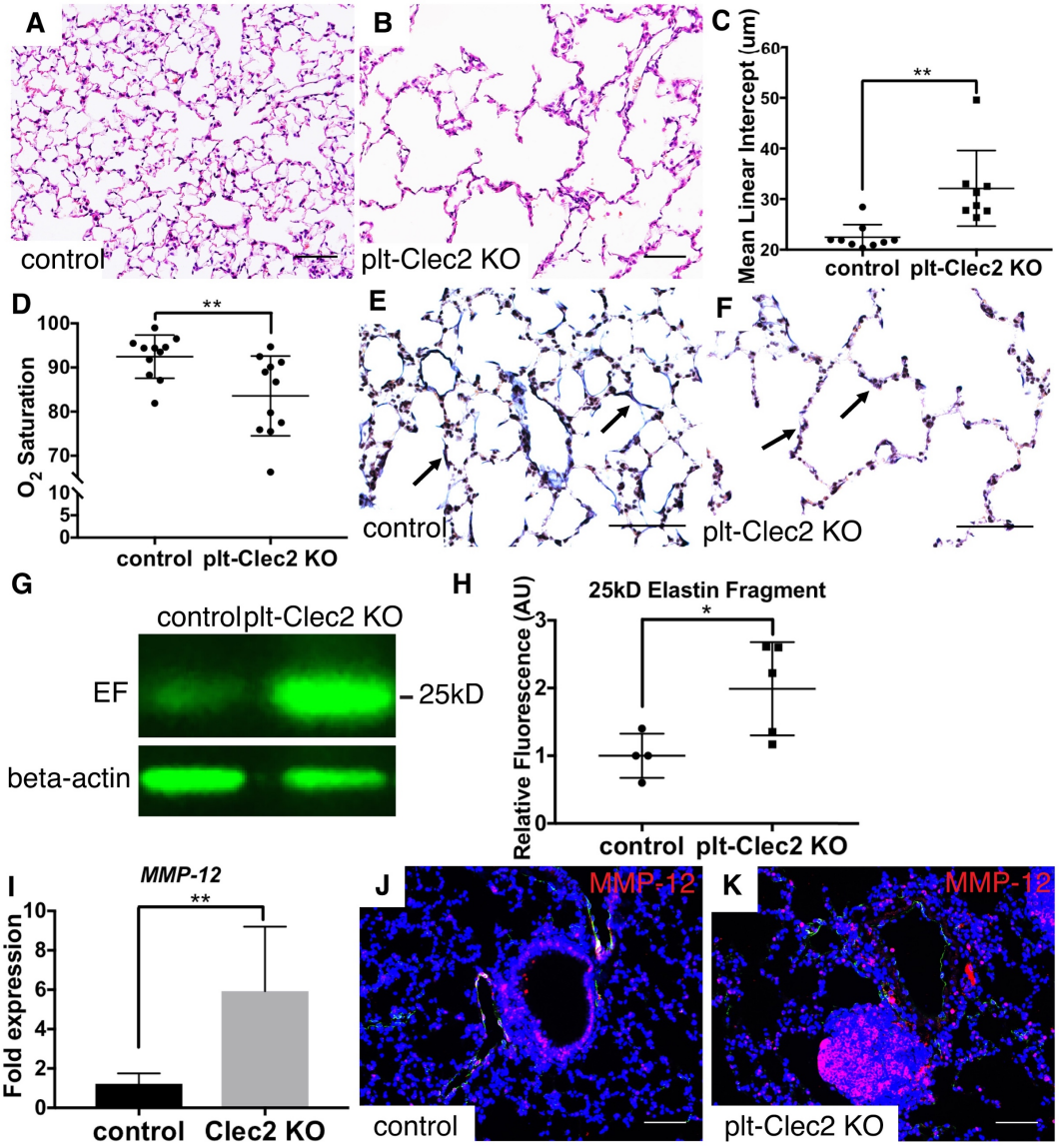

Figure 8: CLEC2 deficiency results in reduced lung function associated with emphysematous changes. (A,B) H&E staining of lung tissue from 6-8 month-old plt-Clec2 KO and control mice. (C) Quantification of alveolar enlargement in 6-8 month old plt-Clec2 KO and control mice by mean linear intercept (MLI). (D) Oxygen saturation in 6-8 month old plt-Clec2 KO and control mice. (E,F) Van Gieson staining for elastin (black, arrows) in the lungs of control and plt-Clec2 KO mice. (G) Western blot of whole lung tissue for 25kD elastin fragment (EF) in 6-8 month-old plt-Clec2 KO and control mice. (H) Quantification of 25kD EF in western blots by fluorescence intensity (AU). Comparisons were made between matched littermates. (I) Quantitative PCR of lung tissue from plt-Clec2 KO and control mice for MMP-12. Comparisons were made between matched littermates. (J,K) Immunohistochemistry for MMP-12 (red) in lungs from plt-Clec2 KO and control mice. Data representative of at least 4 mice in each group. Scale bars = 25μm. All values are means ± SEM. *P* value calculated by Student's *t* test. * $P < 0.05$ ** $P < 0.01$.

References

1. Rafii S, Butler JM, and Ding BS. Angiocrine functions of organ-specific endothelial cells. *Nature.* 2016;529(7586):316-25.
2. Jakus Z, Gleghorn JP, Enis DR, Sen A, Chia S, Liu X, et al. Lymphatic function is required prenatally for lung inflation at birth. *J Exp Med.* 2014;211(5):815-26.
3. Mackersie RC, Christensen J, and Lewis FR. The role of pulmonary lymphatics in the clearance of hydrostatic pulmonary edema. *J Surg Res.* 1987;43(6):495-504.
4. Patterson GA, Mitzner WA, and Sylvester JT. Assessment of fluid balance in isolated sheep lungs. *J Appl Physiol (1985).* 1985;58(3):882-91.
5. Rossler A, Fink M, Goswami N, and Batzel JJ. Modeling of hyaluronan clearance with application to estimation of lymph flow. *Physiol Meas.* 2011;32(8):1213-38.
6. Bakocević N, Worbs T, Davalos-Misslitz A, and Förster R. T cell-dendritic cell interaction dynamics during the induction of respiratory tolerance and immunity. *J Immunol.* 2010;184(3):1317-27.
7. Cook DN, and Bottomly K. Innate immune control of pulmonary dendritic cell trafficking. *Proc Am Thorac Soc.* 2007;4(3):234-9.
8. Stranford S, and Ruddle NH. Follicular dendritic cells, conduits, lymphatic vessels, and high endothelial venules in tertiary lymphoid organs: Parallels with lymph node stroma. *Front Immunol.* 2012;3:350.
9. Jones GW, Hill DG, and Jones SA. Understanding Immune Cells in Tertiary Lymphoid Organ Development: It Is All Starting to Come Together. *Front Immunol.* 2016;7:401.
10. Aloisi F, and Pujol-Borrell R. Lymphoid neogenesis in chronic inflammatory diseases. *Nat Rev Immunol.* 2006;6(3):205-17.
11. Baluk P, Adams A, Phillips K, Feng J, Hong YK, Brown MB, et al. Preferential lymphatic growth in bronchus-associated lymphoid tissue in sustained lung inflammation. *Am J Pathol.* 2014;184(5):1577-92.
12. El-Chemaly S, Levine SJ, and Moss J. Lymphatics in lung disease. *Ann N Y Acad Sci.* 2008;1131:195-202.
13. Hess PR, Rawnsley DR, Jakus Z, Yang Y, Sweet DT, Fu J, et al. Platelets mediate lymphovenous hemostasis to maintain blood-lymphatic separation throughout life. *J Clin Invest.* 2014;124(1):273-84.
14. Maby-El Hajjami H, and Petrova TV. Developmental and pathological lymphangiogenesis: from models to human disease. *Histochem Cell Biol.* 2008;130(6):1063-78.
15. Mislin H. Active contractility of the lymphangion and coordination of lymphangion chains. *Experientia.* 1976;32(7):820-2.
16. Schmid-Schonbein GW. Microlymphatics and lymph flow. *Physiol Rev.* 1990;70(4):987-1028.
17. Gashev AA, Davis MJ, Delp MD, and Zawieja DC. Regional variations of contractile activity in isolated rat lymphatics. *Microcirculation.* 2004;11(6):477-92.
18. Gashev AA. Lymphatic vessels: pressure- and flow-dependent regulatory reactions. *Ann N Y Acad Sci.* 2008;1131:100-9.
19. Zawieja DC. Contractile physiology of lymphatics. *Lymphat Res Biol.* 2009;7(2):87-96.

20. Albelda SM, Hansen-Flaschen JH, Lanken PN, and Fishman AP. Effects of increased ventilation on lung lymph flow in unanesthetized sheep. *J Appl Physiol (1985).* 1986;60(6):2063-70.
21. Pearse DB, Searcy RM, Mitzner W, Permutt S, and Sylvester JT. Effects of tidal volume and respiratory frequency on lung lymph flow. *J Appl Physiol (1985).* 2005;99(2):556-63.
22. Grimbert FA, Martin D, Parker JC, and Taylor AE. Lymph flow during increases in pulmonary blood flow and microvascular pressure in dogs. *Am J Physiol.* 1988;255(5 Pt 2):H1149-55.
23. Choi I, Chung HK, Ramu S, Lee HN, Kim KE, Lee S, et al. Visualization of lymphatic vessels by Prox1-promoter directed GFP reporter in a bacterial artificial chromosome-based transgenic mouse. *Blood.* 2011;117(1):362-5.
24. Meinecke AK, Nagy N, Lago GD, Kirmse S, Klose R, Schrodter K, et al. Aberrant mural cell recruitment to lymphatic vessels and impaired lymphatic drainage in a murine model of pulmonary fibrosis. *Blood.*119(24):5931-42.
25. El-Chemaly S, Malide D, Zudaire E, Ikeda Y, Weinberg BA, Pacheco-Rodriguez G, et al. Abnormal lymphangiogenesis in idiopathic pulmonary fibrosis with insights into cellular and molecular mechanisms. *Proc Natl Acad Sci U S A.* 2009;106(10):3958-63.
26. Mori M, Andersson CK, Graham GJ, Lofdahl CG, and Erjefalt JS. Increased number and altered phenotype of lymphatic vessels in peripheral lung compartments of patients with COPD. *Respir Res.* 2013;14:65.
27. Suzuki-Inoue K, Inoue O, Ding G, Nishimura S, Hokamura K, Eto K, et al. Essential in vivo roles of the C-type lectin receptor CLEC-2: embryonic/neonatal lethality of CLEC-2-deficient mice by blood/lymphatic misconnections and impaired thrombus formation of CLEC-2-deficient platelets. *J Biol Chem.* 2010;285(32):24494-507.
28. Bertozzi CC, Schmaier AA, Mericko P, Hess PR, Zou Z, Chen M, et al. Platelets regulate lymphatic vascular development through CLEC-2-SLP-76 signaling. *Blood.* 2010;116(4):661-70.
29. Sweet DT, Jimenez JM, Chang J, Hess PR, Mericko-Ishizuka P, Fu J, et al. Lymph flow regulates collecting lymphatic vessel maturation in vivo. *J Clin Invest.* 2015;125(8):2995-3007.
30. Benezech C, Nayar S, Finney BA, Withers DR, Lowe K, Desanti GE, et al. CLEC-2 is required for development and maintenance of lymph nodes. *Blood.* 2014;123(20):3200-7.
31. Osada M, Inoue O, Ding G, Shirai T, Ichise H, Hirayama K, et al. Platelet activation receptor CLEC-2 regulates blood/lymphatic vessel separation by inhibiting proliferation, migration, and tube formation of lymphatic endothelial cells. *J Biol Chem.* 2012;287(26):22241-52.
32. Hayakawa T, Furusawa, T., Yamashita, H. A Comparative Anatomical Study of the Lymphatic System of the Lung in Mammals: 5. Findings in Rodentia. *Okajimas Folia Anat Jpn.* 1986;63(2-3):73-80.
33. Cui Y, Liu K, Monzon-Medina ME, Padera RF, Wang H, George G, et al. Therapeutic lymphangiogenesis ameliorates established acute lung allograft rejection. *J Clin Invest.*125(11):4255-68.

34. Legge KL, and Braciale TJ. Accelerated migration of respiratory dendritic cells to the regional lymph nodes is limited to the early phase of pulmonary infection. *Immunity.* 2003;18(2):265-77.
35. Vermaelen K, and Pauwels R. Accelerated airway dendritic cell maturation, trafficking, and elimination in a mouse model of asthma. *Am J Respir Cell Mol Biol.* 2003;29(3 Pt 1):405-9.
36. Yadava K, Bollyky P, and Lawson MA. The formation and function of tertiary lymphoid follicles in chronic pulmonary inflammation. *Immunology.* 2016;149(3):262-9.
37. Ager A. High Endothelial Venules and Other Blood Vessels: Critical Regulators of Lymphoid Organ Development and Function. *Front Immunol.* 2017;8:45.
38. Acton SE, Astarita JL, Malhotra D, Lukacs-Kornek V, Franz B, Hess PR, et al. Podoplanin-rich stromal networks induce dendritic cell motility via activation of the C-type lectin receptor CLEC-2. *Immunity.* 2012;37(2):276-89.
39. Starling EH. On the Absorption of Fluids from the Connective Tissue Spaces. *J Physiol.* 1896;19(4):312-26.
40. Michel CC. Starling: the formulation of his hypothesis of microvascular fluid exchange and its significance after 100 years. *Exp Physiol.* 1997;82(1):1-30.
41. Bland RD, Hansen TN, Haberkern CM, Bressack MA, Hazinski TA, Raj JU, et al. Lung fluid balance in lambs before and after birth. *J Appl Physiol Respir Environ Exerc Physiol.* 1982;53(4):992-1004.
42. Sakuma T, Pittet JF, Jayr C, and Matthay MA. Alveolar liquid and protein clearance in the absence of blood flow or ventilation in sheep. *J Appl Physiol (1985).* 1993;74(1):176-85.
43. Uhley HN, Leeds SE, Sampson JJ, and Friedman M. Role of pulmonary lymphatics in chronic pulmonary edema. *Circ Res.* 1962;11:966-70.
44. Moessinger AC, Harding R, Adamson TM, Singh M, and Kiu GT. Role of lung fluid volume in growth and maturation of the fetal sheep lung. *J Clin Invest.* 1990;86(4):1270-7.
45. Jennrich S, Lee MH, Lynn RC, Dewberry K, and Debes GF. Tissue exit: a novel control point in the accumulation of antigen-specific CD8 T cells in the influenza a virus-infected lung. *J Virol.* 2012;86(7):3436-45.
46. Buch T, Heppner FL, Tertilt C, Heinen TJ, Kremer M, Wunderlich FT, et al. A Cre-inducible diphtheria toxin receptor mediates cell lineage ablation after toxin administration. *Nat Methods.* 2005;2(6):419-26.
47. Martinez-Corral I, Stanczuk L, Frye M, Ulvmar MH, Dieguez-Hurtado R, Olmeda D, et al. Vegfr3-CreER (T2) mouse, a new genetic tool for targeting the lymphatic system. *Angiogenesis.* 2016;19(3):433-45.
48. Dashkevich A, Heilmann C, Kayser G, Germann M, Beyersdorf F, Passlick B, et al. Lymph angiogenesis after lung transplantation and relation to acute organ rejection in humans. *Ann Thorac Surg.* 2010;90(2):406-11.
49. Ruggiero R, Fietsam R, Jr., Thomas GA, Muz J, Farris RH, Kowal TA, et al. Detection of canine allograft lung rejection by pulmonary lymphoscintigraphy. *J Thorac Cardiovasc Surg.* 1994;108(2):253-8.
50. Bracke KR, Verhamme FM, Seys LJ, Bantsimba-Malanda C, Cunoosamy DM, Herbst R, et al. Role of CXCL13 in cigarette smoke-induced lymphoid follicle formation and chronic obstructive pulmonary disease. *Am J Respir Crit Care Med.* 2013;188(3):343-55.

51. Jia J, Conlon TM, Sarker RS, Tasdemir D, Smirnova NF, Srivastava B, et al. Cholesterol metabolism promotes B-cell positioning during immune pathogenesis of chronic obstructive pulmonary disease. *EMBO Mol Med.* 2018;10(5).
52. Mund SI, Stampanoni M, and Schittny JC. Developmental alveolarization of the mouse lung. *Dev Dyn.* 2008;237(8):2108-16.
53. Molet S, Belleguic C, Lena H, Germain N, Bertrand CP, Shapiro SD, et al. Increase in macrophage elastase (MMP-12) in lungs from patients with chronic obstructive pulmonary disease. *Inflamm Res.* 2005;54(1):31-6.
54. Sandhaus RA, and Turino G. Neutrophil elastase-mediated lung disease. *COPD.* 2013;10 Suppl 1:60-3.
55. Stolz D, Leeming DJ, Kristensen JHE, Karsdal MA, Boersma W, Louis R, et al. Systemic Biomarkers of Collagen and Elastin Turnover Are Associated With Clinically Relevant Outcomes in COPD. *Chest.* 2017;151(1):47-59.
56. Houghton AM, Quintero PA, Perkins DL, Kobayashi DK, Kelley DG, Marconcini LA, et al. Elastin fragments drive disease progression in a murine model of emphysema. *J Clin Invest.* 2006;116(3):753-9.
57. Hunninghake GW, Davidson JM, Rennard S, Szapiel S, Gadek JE, and Crystal RG. Elastin fragments attract macrophage precursors to diseased sites in pulmonary emphysema. *Science.* 1981;212(4497):925-7.
58. Sellami M, Meghraoui-Kheddar A, Terryn C, Fichel C, Bouland N, Diebold MD, et al. Induction and regulation of murine emphysema by elastin peptides. *Am J Physiol Lung Cell Mol Physiol.* 2016;310(1):L8-23.
59. Hautamaki RD, Kobayashi DK, Senior RM, and Shapiro SD. Requirement for macrophage elastase for cigarette smoke-induced emphysema in mice. *Science.* 1997;277(5334):2002-4.
60. Demedts IK, Morel-Montero A, Lebecque S, Pacheco Y, Cataldo D, Joos GF, et al. Elevated MMP-12 protein levels in induced sputum from patients with COPD. *Thorax.* 2006;61(3):196-201.
61. Wong BW, Zecchin A, García-Caballero M, and Carmeliet P. Emerging Concepts in Organ-Specific Lymphatic Vessels and Metabolic Regulation of Lymphatic Development. *Dev Cell.* 2018;45(3):289-301.
62. Karkkainen MJ, Haiko P, Sainio K, Partanen J, Taipale J, Petrova TV, et al. Vascular endothelial growth factor C is required for sprouting of the first lymphatic vessels from embryonic veins. *Nat Immunol.* 2004;5(1):74-80.
63. Huxley VH, and Scallan J. Lymphatic fluid: exchange mechanisms and regulation. *J Physiol.* 2011;589(Pt 12):2935-43.
64. Rangel-Moreno J, Hartson L, Navarro C, Gaxiola M, Selman M, and Randall TD. Inducible bronchus-associated lymphoid tissue (iBALT) in patients with pulmonary complications of rheumatoid arthritis. *J Clin Invest.* 2006;116(12):3183-94.
65. Sato M, Hirayama S, Hwang DM, Lara-Guerra H, Wagnetz D, Waddell TK, et al. The role of intrapulmonary de novo lymphoid tissue in obliterative bronchiolitis after lung transplantation. *J Immunol.* 2009;182(11):7307-16.
66. Coxson HO, Dirksen A, Edwards LD, Yates JC, Agusti A, Bakke P, et al. The presence and progression of emphysema in COPD as determined by CT scanning and biomarker

expression: a prospective analysis from the ECLIPSE study. *Lancet Respir Med.* 2013;1(2):129-36.
67. Paris AJ, Liu Y, Mei J, Dai N, Guo L, Spruce LA, et al. Neutrophils promote alveolar epithelial regeneration by enhancing type II pneumocyte proliferation in a model of acid-induced acute lung injury. *Am J Physiol Lung Cell Mol Physiol.* 2016;311(6):L1062-L75.
68. Wang C, de Mochel NSR, Christenson SA, Cassandras M, Moon R, Brumwell AN, et al. Expansion of hedgehog disrupts mesenchymal identity and induces emphysema phenotype. *J Clin Invest.* 2018.